

Revision 1

**Correianevesite, $\text{Fe}^{2+}\text{Mn}^{2+}_2(\text{PO}_4)_2 \cdot 3\text{H}_2\text{O}$, a new reddingite-group
mineral from the Cigana mine, Conselheiro Pena, Minas Gerais,
Brazil**

**Nikita V. Chukanov^{1*}, Ricardo Scholz², Natalia V. Zubkova³, Igor V. Pekov³, Dmitriy I.
Belakovskiy⁴, Konstantin V. Van⁵, Leonardo Lagoeiro², Leonardo M. Graça², Klaus
Krambrock⁶, Luiz C.A. de Oliveira⁷, Luiz A.D. Menezes Filho⁸, Mário L.S.C. Chaves⁸ and
Dmitriy Y. Pushcharovsky³**

¹Institute of Problems of Chemical Physics, Russian Academy of Sciences, Chernogolovka,
Moscow Region 142432, Russia

²Universidade Federal de Ouro Preto (UFOP), Escola de Minas, Departamento de Geologia,
Campus Morro do Cruzeiro, 35400-000, Ouro Preto, MG, Brazil

³Faculty of Geology, Moscow State University, Vorobievsky Gory, Moscow, 119991 Russia

⁴Fersman Mineralogical Museum, Russian Academy of Sciences, Leninskiy Prospekt 18-2,
Moscow, 119071 Russia

⁵Institute of Experimental Mineralogy, Russian Academy of Sciences, Chernogolovka, Moscow
Region 142432, Russia

⁶Universidade Federal de Minas Gerais, Instituto de Ciências Exatas, Departamento de Física,
Avenida Antônio Carlos, 6627, 31270-901, Belo Horizonte, MG, Brazil

⁷Universidade Federal de Minas Gerais, Instituto de Ciências Exatas, Departamento de Química,
Avenida Antônio Carlos, 6627, 31270-901, Belo Horizonte, MG, Brazil

⁸Universidade Federal de Minas Gerais, Instituto de Geociências, Departamento de Geologia,
Avenida Antônio Carlos, 6627, 31270-901, Belo Horizonte, MG, Brazil

*chukanov@icp.ac.ru

31
32
33
34
35
36
37
38
39
40
41
42
43
44
45
46
47
48
49
50
51
52
53
54
55
56
57

ABSTRACT

Correianevesite, ideally $\text{Fe}^{2+}\text{Mn}^{2+}_2(\text{PO}_4)_2 \cdot 3\text{H}_2\text{O}$, is a new reddingite-group mineral approved by the CNMNC (IMA 2013-007). It occurs in a phosphate-rich granite pegmatite outcropped by the Cigana mine, Conselheiro Pena, Rio Doce valley, Minas Gerais, Brazil. Associated minerals are: triphylite, lithiophilite, frondelite, rockbridgeite, eosphorite, vivianite, fairfieldite, leucophosphite, cyrilovite, phosphosiderite, etc. Correianevesite occurs as grayish-brown to reddish-brown transparent bipyramidal crystals up to 4 mm in size. The streak is white, and the luster is vitreous. Mohs' hardness is $3\frac{1}{2}$. Cleavage is poor on (010). Fracture is laminated, uneven across cleavage. The measured density is $3.25(2) \text{ g cm}^{-3}$; the calculated density is 3.275 g cm^{-3} . The mineral is biaxial (+), $\alpha = 1.661(5)$, $\beta = 1.673(5)$, $\gamma = 1.703(5)$, $2V_{\text{meas}} = 70(10)^\circ$, $2V_{\text{calc}} = 65.6^\circ$. The IR spectrum confirms the presence of H_2O . The Mössbauer spectrum shows the presence of two sites for Fe^{2+} and one site for Fe^{3+} occupied in the ratio $\text{Fe}^{12+}:\text{Fe}^{22+}:\text{Fe}^{3+} = 39:55:6$. The chemical composition is (electron microprobe, H_2O determined by gas chromatography of ignition products, Fe apportioned between FeO and Fe_2O_3 based on Mössbauer data, wt.%): MnO 29.21, FeO 21.74 Fe_2O_3 1.54, P_2O_5 34.59, H_2O 12.6, total 99.68. The empirical formula, based on 11 O *apfu*, is $\text{H}_{5.78}\text{Mn}_{1.70}\text{Fe}^{2+}_{1.25}\text{Fe}^{3+}_{0.08}\text{P}_{2.015}\text{O}_{11}$. The strongest lines of the powder X-ray diffraction pattern [d , Å (I , %) (hkl)] are: 5.08 (43) (020), 4.314 (28) (002, 210), 3.220 (100) (221, 202), 3.125 (25) (122), 2.756 (35) (103, 230), 2.686 (25) (222, 113), 2.436 (22) (123) and 2.233 (23) (411, 331). The crystal structure is solved ($R_I = 0.0176$). Correianevesite is orthorhombic, space group *Pbna*, $a = 9.4887(2)$, $b = 10.1149(2)$, $c = 8.7062(2)$ Å, $V = 835.60(3)$ Å³, $Z = 4$. The refined crystal-chemical formula is: $(\text{Fe}^{2+}_{0.72}\text{Mn}^{2+}_{0.20}\text{Fe}^{3+}_{0.08})(\text{Mn}_{1.48}\text{Fe}^{2+}_{0.52})(\text{PO}_4)_2(\text{H}_2\text{O},\text{OH})_3$.

Keywords: correianevesite, new mineral, phosphate, reddingite group, Cigana mine, Conselheiro Pena, Rio Doce valley, Minas Gerais, Brazil, crystal structure, Mössbauer spectroscopy.

58

INTRODUCTION

59

60 Correianevesite is a new mineral approved by the IMA Commission on New Minerals,
61 Nomenclature and Classification (IMA no. 2013-007). It was discovered in a granite pegmatite
62 outcropped by the Cigana mine (Lavra da Cigana; formerly known as João mine), Rio Doce
63 valley, Conselheiro Pena county, Minas Gerais, Brazil. The pegmatite belongs to the Conselheiro
64 Pena pegmatite district, Eastern Brazilian pegmatite province known for a wide diversity of
65 phosphate minerals (Pedrosa et al. 2011).

66 The Cigana pegmatite is mined out and in the past was mined for industrial feldspar and with
67 minor importance gemstones and samples for the collectors market. The pegmatite is heterogeneous
68 with well-developed mineralogical and textural zoning. It has symmetric lens shape with the longer
69 axis trending to NW-SE and the body dipping subvertically. The extension is at least 50 m, and the
70 thickness is up to 20 m. The pegmatite is hosted by quartz-mica schist with garnet, staurolite and
71 sillimanite of the São Tomé Formation. Hydrothermal and metasomatic fluids were responsible for
72 the albitization, the development of miarolitic cavities, and the formation of a complex secondary
73 phosphate assemblage described by Chaves et al. (2005).

74 The primary mineral association is represented by quartz, muscovite, microcline, schorl,
75 almandine-spessartine, spodumene and triphylite. The secondary association is mainly composed by
76 albite, Ta and Nb oxides, hydrothermal beryl, cassiterite, pyrite and numerous phosphates formed as
77 a result of alteration of triphylite (Chaves et al. 2005). The paragenetic assemblage of secondary
78 phosphates is composed by lithiophilite, correianevesite, hureaulite, frondelite, fluorapatite,
79 eosphorite, fairfieldite, gormanite, and vivianite.

80 The new mineral is named in memory of Professor José Marques Correia Neves (1929-2011),
81 professor of the Instituto de Geociências, Universidade Federal de Minas Gerais, who was the most
82 active geoscientist in the study of Brazilian pegmatites, especially in the region of Conselheiro Pena

83 and Araçuaí, as well as in Alto Ligonha in Mozambique, where he discovered hafnon, the Hf
84 analogue of zircon.

85 The type specimen of correianevesite (a part of the holotype) is deposited in the mineralogical
86 collections of the Museu de Ciência e Técnica, Escola de Minas, Universidade Federal de Ouro
87 Preto, Praça Tiradentes, Centro, 35400-000 – Ouro Preto, MG, Brazil, with the registration number
88 SAA-081B.

89

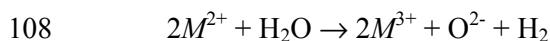
90 **GENERAL APPEARANCE AND PHYSICAL PROPERTIES**

91

92 Correianevesite occurs as light grayish-brown to reddish-brown transparent bipyramidal
93 crystals up to 4 mm in size (Figure 1) in cavities of triphylite. The only form observed is {111}. The
94 streak is white, and the luster is vitreous. The mineral is non-fluorescent under ultraviolet light.
95 Mohs' hardness is 3½. Cleavage is poor on (010). Fracture is laminated, uneven across cleavage.
96 The density measured by flotation in heavy liquids is 3.25(2) g cm⁻³. The calculated density is 3.275
97 g cm⁻³ based on the empirical formula and unit-cell parameters obtained from the single-crystal X-
98 ray diffraction data.

99 Thermal data for correianevesite were obtained using a Shimadzu analyzer in a nitrogen
100 atmosphere, at a gas flow rate of 50 cm³ min⁻¹. Differential thermal analysis (DTA) and
101 thermogravimetric (TG) analyses were carried out simultaneously. Crushed samples with 14.88 mg
102 weight were heated in an open platinum crucible at a rate of 10°C min⁻¹ up to a temperature of
103 800°C. The TG curve of correianevesite in nitrogen atmosphere is given in Figure 2.

104 The lowered weight loss of 10.45 % obtained by TG, as compared with H₂O content of 12.6
105 wt.% obtained by gas chromatography of products of ignition (see below), is explained by self-
106 oxidation (a phenomenon typical of Fe²⁺- and Mn²⁺-phosphates: see e.g. Frost et al. 2004;
107 Chukanov et al. 2012), in accordance with the following simplified schemes (*M* = Fe, Mn):



110 These processes correspond to exothermic effects in the DTA curve (Figure 3) and may be
111 explained by the partial oxidation of Fe^{2+} to Fe^{3+} .

112 In order to obtain infrared (IR) absorption spectrum, correianevesite powder was mixed with
113 anhydrous KBr, pelletized, and analysed using an ALPHA FTIR spectrometer (Bruker Optics) at
114 the resolution of 4 cm^{-1} and number of scans of 16. IR spectrum of analogous pellet of pure
115 KBr was used as a reference.

116 Absorption bands in the IR spectrum of correianevesite (Figure 4) and their assignments are
117 (cm^{-1} ; s – strong band, w – weak band, sh – shoulder): 3457, 3200 (O–H stretching vibrations of H_2O
118 molecules and OH^- anions, hydrogen bonds of medium strengths), 2530, 2033w, 1890 (vibrations of
119 the fragments O–H \cdots O–P, very strong hydrogen bonds of acidic OH groups), 2247w (overtone of
120 asymmetric stretching vibrations of PO_4^{3-} anions), 1636w, 1575 (bending vibrations of H_2O
121 molecules), 1054s, 1013s (asymmetric stretching vibrations of PO_4^{3-} anions), 758, 750sh, 661
122 (librational vibrations of H_2O molecules forming strong hydrogen bonds), 598, 570, 555sh (O–P–O
123 bending vibrations of PO_4^{3-} anions), 476w, 417w, 384w (mixed lattice vibrations).

124 Bands of B-, C- and N-bearing groups are absent in the IR spectrum of correianevesite. The
125 nature of anomalously strong hydrogen bonds is discussed below.

126 The IR spectrum of correianevesite is comparable to those of the isostructural minerals
127 phosphoferrite and reddingite.

128 Mössbauer spectra were collected in constant acceleration transmission mode with a 10 mCi
129 $^{57}\text{Co/Rh}$ source at 25 and 298 K. The data were stored in a 1024-channel MCS memory unit and
130 were fitted using Lorentzian line shapes with a least-squares fitting procedure using the NORMOS
131 program. Isomer shifts were calculated relatively to $\alpha\text{-Fe}$.

132 According to Mössbauer spectroscopy data (Figure 5, Table 1), correianevesite contains three
133 kinds of iron cations (two bivalent and one trivalent) having 6-fold coordination and present in the
134 atomic proportions $\text{Fe}^{1^{2+}}:\text{Fe}^{2^{2+}}:\text{Fe}^{3^{2+}} = 39:55:6$.

135

136 Correianevesite is optically biaxial (+), $\alpha = 1.661(5)$, $\beta = 1.673(5)$, $\gamma = 1.703(5)$, $2V_{\text{meas}} =$
137 $70(10)^\circ$, $2V_{\text{calc}} = 65.6^\circ$. Dispersion of optical axes is strong, $r > v$. The mineral is nonpleochroic,
138 colourless under the microscope.

139

140

CHEMICAL COMPOSITION

141

142 Seven point analyses were carried out using VEGA TS 5130MM SEM equipped with
143 EDX analyser (INCA Si(Li) detector), at an operating voltage of an electron microprobe of 20 kV
144 and a beam current of 0.5 nA. The beam was rasterized on an area 16 x 16 μm to minimise unstable
145 sample damage. Attempts to use WDS mode, with higher beam current, were unsuccessful because
146 of the instability of the mineral containing water. The contents of F, Na, Mg, Al, Si, S, K, Ca, Ti,
147 Zn and As are below their detection limits. H_2O was analysed by gas chromatography of products
148 of ignition at 1200°C . CO_2 was not analysed because of the absence of absorption bands
149 corresponding to vibrations of C-O bonds in the IR spectrum. Analytical data are given in Table 2.

150 The empirical formula based on 11 O atoms is $\text{H}_{5.78}\text{Mn}_{1.70}\text{Fe}^{2+}_{1.25}\text{Fe}^{3+}_{0.08}\text{P}_{2.015}\text{O}_{11}$. The
151 simplified formula is $\text{Fe}^{2+}\text{Mn}^{2+}_2(\text{PO}_4)_2 \cdot 3\text{H}_2\text{O}$, which requires MnO 34.63, FeO 17.54, P_2O_5 34.64,
152 H_2O 13.19, total 100.00 wt%.

153 The Gladstone-Dale compatibility between chemical data, refractive indices and density is (1-
154 K_p/K_c) = 0.013 (superior).

155

156

X-RAY DIFFRACTION DATA AND CRYSTAL STRUCTURE

157

158 The X-ray powder-diffraction data (Table 3) were collected with a STOE IPDS II single-
159 crystal diffractometer equipped with an Image Plate detector using the Gandolfi method by
160 employing the $\text{MoK}\alpha$ radiation and a sample-detector distance of 200 mm. Orthorhombic unit-cell
161 parameters refined from the powder data are as follows: $a = 9.491(7)$, $b = 10.121(7)$, $c = 8.721(9)$

162 Å, $V = 838(2) \text{ \AA}^3$. Measured interplanar spacings and intensities of observed reflections are in a
163 good agreement with corresponding values calculated from the crystal structure.

164 Single-crystal X-ray diffraction measurements were made with a single-crystal Xcalibur S
165 diffractometer equipped with a CCD detector. Absorption correction was applied according to the
166 shape of the crystal. The structure was solved by direct methods and refined anisotropically using
167 SHELXS-97 and SHELXL-97 (Sheldrick, 2008), respectively, to $R = 0.0176$ for 1662 unique
168 reflections with $I > 2\sigma(I)$ in space group *Pbna*. All hydrogen atoms of two water molecules were
169 found and refined.

170 The structure model is in a good agreement with those of the other reddingite-group minerals.
171 A small amount of Mn was added to the Fe-dominant $M(1)$ site, and a small amount of Fe was added
172 to the Mn-dominant $M(2)$ site according to the results of the refinement of electronic composition of
173 the site, chemical and Mössbauer data. The occupancy coefficients of the cations in $M(1)$ and $M(2)$
174 sites were fixed in the final stages of the refinement. The crystallographic characteristics of the
175 mineral, the details of the X-ray diffraction study and the structure-refinement parameters are given
176 in Table 4, atom coordinates and equivalent thermal displacement parameters – in Table 5,
177 anisotropic displacement parameters – in Table 6 and selected interatomic distances – in Table 7.

178 Like other representatives of the phosphoferrite structure type, correianevesite contains (100)
179 octahedral layers (Figure 6) formed by the parallel to the c axis chains of edge-sharing dimers of
180 $M(2)O_4(H_2O)_2$ polyhedra connected *via* common edges with isolated from each other
181 $M(1)O_4(H_2O)_2$ octahedra. Adjacent chains are connected with each other by the corners of $M(2)$
182 octahedra. The neighbouring octahedral layers are connected by PO_4 tetrahedra (Figure 7).

183

184 **DISCUSSION AND IMPLICATIONS**

185

186 The comparative crystal chemistry of different minerals with the phosphoferrite structure type
187 has been discussed by Moore et al. (1980). All these minerals are orthorhombic phosphates with the

188 general formula $M(1)M(2)_2(\text{PO}_4)_2(\text{OH},\text{H}_2\text{O})_3$ where octahedral sites $M(1)$ and $M(2)$ can contain
189 Mn^{2+} , Fe^{2+} , Mg and Fe^{3+} (Table 8) with minor admixtures of Ca and Al and some other (trace)
190 components. Mn^{2+} preferably occupies the larger octahedron $M(2)$, but in reddingite both $M(1)$ and
191 $M(2)$ sites are dominantly occupied by Mn^{2+} .

192 Based on interatomic distances and observed trends in site populations, Moore et al. (1980)
193 assumed the existence of a hypothetical reddingite-group mineral with the end-member formula
194 $\text{Fe}^{2+}\text{Mn}^{2+}_2(\text{PO}_4)_2 \cdot 3\text{H}_2\text{O}$, in which Fe^{2+} occupies the $M(1)$ site and Mn^{2+} occupies the $M(2)$ site. The
195 discovery of correianevesite confirmed this assumption.

196 Taking into account Mössbauer spectroscopy data (Table 1), the results of the crystal structure
197 refinement (Tables 5, 6), compositional data (Table 2) and general trends in the cation distribution
198 between the sites $M(1)$ and $M(2)$ (Moore et al. 1980), the crystal-chemical formula of
199 correianevesite can be written as $(\text{Fe}^{2+}_{0.72}\text{Mn}^{2+}_{0.20}\text{Fe}^{3+}_{0.08})(\text{Mn}_{1.48}\text{Fe}^{2+}_{0.52})(\text{PO}_4)_2(\text{H}_2\text{O},\text{OH})_3$. This
200 formula was derived assuming that the major part of Fe^{2+} (corresponding to $\text{Fe}1^{2+}$, by Mössbauer
201 data) occupies the smaller octahedron $M(1)$. Note that, according to the assumption that $\text{Fe}1^{2+}$
202 corresponds to bivalent iron in the $M(2)$ site, the crystal chemical formula would be
203 $(\text{Fe}^{2+}_{0.52}\text{Mn}^{2+}_{0.41}\text{Fe}^{3+}_{0.08})(\text{Mn}^{2+}_{1.29}\text{Fe}^{2+}_{0.73})(\text{PO}_4)_2(\text{H}_2\text{O},\text{OH})_3$ and also would correspond to a mineral
204 with the end-member formula $\text{Fe}^{2+}\text{Mn}^{2+}_2(\text{PO}_4)_2 \cdot 3\text{H}_2\text{O}$. However, the latter variant of cation
205 distribution is hardly probable taking into account cation-anion distances.

206 Comparative data for correianevesite and related minerals are given in Table 9. It is important
207 to note that landesite and correianevesite cannot be distinguished by electron microprobe analysis,
208 but landesite is characterized by much higher values of refractive indexes as a result of high Fe^{3+}
209 content. Correianevesite and Fe-bearing reddingite can be distinguished only by means of
210 Mössbauer spectroscopy.

211 The presence of acidic OH groups detected by IR spectroscopy data is due to the asymmetric
212 polarization of H_2O molecules that form strong hydrogen bond $\text{Ow}(2) - \text{H}(2) \cdots \text{O}(1)$ (with the distance
213 $\text{Ow}(2) \cdots \text{O}(1)$ of 2.539 Å) and act as proton donors. This phenomenon is very typical for nominally

214 neutral sulphates, phosphates and arsenates and results in the dynamic acid-base equilibrium $\text{AO}_4^{3-} +$
215 $\text{H}_2\text{O} \leftrightarrow \text{HAO}_4^{2-} + \text{OH}^-$ (A = P, As or S) that is usually shifted towards left side (see *e. g.* Chukanov
216 et al. 2010, 2012; Nestola et al. 2012). Note that the presence of acid phosphate groups in
217 correianevesite (considered as reddingite before Mössbauer data have been obtained) was detected also
218 by means of Raman spectroscopy (Frost et al. 2012). In particular, a strong band at 1007 cm^{-1} was
219 assigned to symmetric stretching vibrations of HOPO_3^{2-} .

220

221

ACKNOWLEDGEMENTS

222

223 We acknowledge Russian Foundation for Basic Researches (grant no. 11-05-00407-a) for
224 financial support, and all members of the IMA Commission on New Minerals, Nomenclature and
225 Classification for their helpful suggestions and comments. Special thanks also to the Brazilian
226 agencies Fapemig and CNPq (CORGEMA II and grant No. 306287/2012-9). We also thank Beda
227 Hofmann, Frederic Hatert and Fabrizio Nestola for useful comments.

228

229

REFERENCES CITED

230

- 231 Chaves, M.L.S.C., Scholz, R., Atencio, D. and Karfunkel, J. (2005) Assembléias e paragêneses
232 minerais singulares nos pegmatitos da região de Galiléia (Minas Gerais). *Geociências*, 24, 143
233 – 161 (in Portuguese).
- 234 Chukanov, N.V., Mukhanova, A.A., Möckel, S., Belakovskiy, D.I., and Levitskaya, L.A. (2010)
235 Nickeltalmessite, $\text{Ca}_2\text{Ni}(\text{AsO}_4)_2 \cdot 2\text{H}_2\text{O}$, a new mineral species of the fairfieldite group, Bou
236 Azzer, Morocco. *Geology of Ore Deposits*, 52, 606-611.
- 237 Chukanov, N.V., Scholz, R., Aksenov, S.M., Rastsvetaeva, R.K., Pekov, I.V., Belakovskiy, D.I.,
238 Krambrock, K., Paniago, R.M., Righi, A., Martins, R.F., Belotti, F.M., and Bermanec, V.
239 (2012) Metavivianite, $\text{Fe}^{2+}\text{Fe}^{3+}_2(\text{PO}_4)_2(\text{OH})_2 \cdot 6\text{H}_2\text{O}$: new data and formula revision.
240 *Mineralogical Magazine* 76, 725-741.
- 241 Feklichev, V.G. (1989) *Diagnostic Constants of Minerals*, 480 p. Nedra, Moscow (in Russian).
- 242 Frost, R.L., Weier, M.L., and Lyon, W. (2004) Metavivianite, an intermediate mineral phase
243 between vivianite, and ferro/ferristrunzite – a Raman spectroscopic study. *Neues Jahrbuch für*
244 *Mineralogie, Monatshefte*, 5, 228-240.
- 245 Frost, L.R., Xi Y., Scholz, R., Belotti, F.M., and Lagoeiro, L.E. (2012) Chemistry, Raman and
246 infrared spectroscopic characterization of the phosphate mineral reddingite:
247 $(\text{Mn,Fe})_3(\text{PO}_4)_2(\text{H}_2\text{O,OH})_3$, a mineral found in lithium-bearing pegmatite. *Physics and*
248 *Chemistry of Minerals*, 39, 803-810.
- 249 Kleber, W., and Donnay, J.D.H. (1961) The heteromorphism of phosphoferrite–reddingite.
250 *Zeitschrift für Kristallografie*, 115, 161-168.
- 251 Moore, P.B. (1964) Investigations of landesite. *American Mineralogist*, 49, 1122-1125.
- 252 Moore, P.B. (1971) The $\text{Fe}^{2+}(\text{H}_2\text{O})_n(\text{PO}_4)_2$ homologous series: crystal-chemical relationships and
253 oxidized equivalents. *American Mineralogist*, 56, 1-17.

- 254 Moore, P.B., and Araki, T. (1976) A mixed-valence solid-solution series: crystal structures of
255 phosphoferrite, $\text{Fe}^{\text{II}}_3(\text{H}_2\text{O})_3[\text{PO}_4]_2$, and kryzhanovskite, $\text{Fe}^{\text{III}}_3(\text{OH})_3[\text{PO}_4]_2$. Inorganic Chemistry,
256 15, 316-321.
- 257 Moore, P.B., Araki, T., and Kampf, A.R. (1980) Nomenclature of the phosphoferrite structure type:
258 refinements of landsite and kryzhanovskite. Mineralogical Magazine, 43, 789-795.
- 259 Nestola, F., Cámara, F., Chukanov, N.V., Atencio, D., Coutinho, J.M.V., Contreira, R.R. Filho &
260 Färber, G. (2012) Witzkeite: a new rare nitrate-sulphate mineral from a guano deposit at Punta
261 de Lobos, Chile. American Mineralogist, 97, 1783-1787.
- 262 Pedrosa-Soares, A.C., Campos, C.M. De, Noce, C.M., Silva, L.C. Da, Novo, T.A., Roncato, J.,
263 Medeiros, S.M., Castañeda, C., Queiroga, G.N., Dantas, E., Dussin, I.A. & Alkmim, F. (2011)
264 Late Neoproterozoic-Cambrian granitic magmatism in Araçuaí orogen (Brazil), the Eastern
265 Brazilian Pegmatite Province and related mineral resources. Geological Society Special
266 Publication, 350, 25-51.
- 267 Sheldrick, G.M. (2008) A short history of *SHELX*. Acta Cryst. A, 64, 112-122.
- 268 Tennyson, C. (1954) Phosphoferrit und Reddingit von Hagedorf. Neues Jahrbuch für Mineralogie,
269 Abhandlungen, 87, 185-217.
- 270

271

FIGURE CAPTIONS

272 Figure 1. Bipyramidal crystals of correianevesite on hureaulite. Field of view: 6 mm. Photo:
273 Carlos Menezes.

274 Figure 2. TG curve of correianevesite obtained in nitrogen atmosphere at a heating rate of
275 $10^{\circ}\text{C min}^{-1}$.

276 Figure 3. DTA curve of correianevesite obtained in nitrogen atmosphere at a heating rate of
277 $10^{\circ}\text{C min}^{-1}$.

278 Figure 4. IR spectrum of powdered correianevesite in KBr pellet.

279 Figure 5. Mössbauer spectrum of correianevesite.

280 Figure 6. Octahedral layer in the structure of correianevesite. $M1O_6$ octahedra are dark, $M2O_6$
281 octahedra are light, H atoms are shown with small circles. Unit cell is outlined.

282 Figure 7. The crystal structure of correianevesite: *ab* projection. Unit cell is outlined.

283

284

285 Table 1. Mössbauer data for correianevesite.
 286

Cation	Isomer shift, mm s ⁻¹	Quadrupole splitting, mm s ⁻¹	Line width, mm s ⁻¹	Area, %
Fe1 ²⁺	1.23(4)	1.63(1)	0.27(2)	39(1)
Fe2 ²⁺	1.23(4)	2.40(9)	0.29(1)	55(3)
Fe ³⁺	0.35(1)	1.20(3)	0.49(5)	6.0(3)

287
 288

289 Table 2. Chemical composition of correianevesite.
 290

Constituent	Content, wt%	Range	Standard deviation	Probable standard
MnO	29.21	27.87-30.14	0.78	MnTiO ₃
FeO ^a	21.74	22.09-24.45 ^b	0.77 ^b	Fe ₂ O ₃
Fe ₂ O ₃ ^a	1.54			
P ₂ O ₅	34.59	34.19-35.02	0.27	LaPO ₄
H ₂ O	12.6±0.1			
Total	99.68			

299 ^aTotal iron content analysed using a microprobe and initially calculated as FeO was 23.13 wt%; it
 300 was apportioned between FeO and Fe₂O₃ (as well as between two sites) based on Mössbauer data
 301 (see Authors' Remarks).

302 ^bFor total iron calculated as FeO.

303
 304
 305

306
307

Table 3. X-ray powder diffraction data for correianevesite.

I_{obs} , %	d_{obs} , Å	I_{calc} , %*	d_{calc} , Å**	hkl
3	6.45	2	6.415	101
19	5.44	20	5.417	111
43	5.08	45	5.057	020
21	4.761	23	4.744	200
28	4.314	4, 27	4.353, 4.295	002, 210
8	3.985	8	3.972	121
4	3.886	2	3.852	211
13	3.471	17	3.460	220
100	3.220	100, 38	3.216, 3.208	221, 202
25	3.125	28	3.116	122
10	2.985	5, 8	2.985, 2.973	131, 301
35	2.756	15, 38	2.775, 2.748	103, 230
25	2.686	12, 29	2.709, 2.676	222, 113
5	2.567	5, 1	2.566, 2.563	132, 321
15	2.484	10, 20	2.517, 2.481	023, 312
22	2.436	29	2.433	123
8	2.355	13	2.353	141
23	2.233	16, 19	2.232, 2.230	411, 331
12	2.184	12, 4	2.187, 2.177	042, 004
13	2.136	3, 16	2.138, 2.131	303, 142
3	2.087	2, 1	2.092, 2.085	313, 421
6	2.040	1, 9	2.040, 2.038	412, 332
14	1.973	2, 18	1.978, 1.970	204, 323
17	1.933	1, 11	1.929, 1.926	151, 341
4	1.855	7	1.854	501
5	1.809	5	1.806	333
2	1.767	4	1.766	314
3	1.740	6	1.741	521
8	1.712	6, 4	1.714, 1.713	512, 105
9	1.649	7, 6, 5	1.650, 1.646, 1.645	044, 025, 522
15	1.630	14	1.630	161
9	1.588	2, 2, 13	1.589, 1.588, 1.587	260, 503, 352
13	1.561	3, 2, 15	1.563, 1.562, 1.558	261, 610, 244
10	1.520	3, 16	1.525, 1.516	305, 451
2	1.491	2	1.495	541
1	1.483	3	1.487	621
2	1.467	1, 4	1.471, 1.466	612, 361
4	1.452	3, 7	1.451, 1.448	006, 434
4	1.423	1, 6	1.426, 1.420	622, 116
4	1.419	1, 1	1.418, 1.416	145, 514
6	1.381	4, 4	1.382, 1.380	270, 126
5	1.340	1, 1, 7	1.342, 1.341, 1.339	354, 640, 701
2	1.320	1, 2	1.319, 1.317	552, 272
2	1.311	2	1.310	462
1	1.299	2	1.295	721
3	1.283	3, 2	1.283, 1.282	264, 173
2	1.273	2, 1	1.279, 1.271	604, 255

1	1.262	1	1.264	080
2	1.242	3	1.240	624
2	1.232	1	1.228	364
3	1.210	1, 2	1.211, 1.210	562, 281
3	1.206	4	1.204	182
2	1.177	2	1.176	282
3	1.170	3	1.170	156
3	1.155	2, 2	1.153, 1.153	660, 455
4	1.147	2, 2	1.151, 1.145	183, 653
1	1.118	1	1.116	822
2	1.107	1, 4	1.108, 1.105	147, 743

308 *For the calculated X-ray powder pattern only reflections with $I_{\text{calc}} \geq 1\%$ are given.

309 **Calculated for unit cell parameters obtained from single-crystal data.

310

311

312 Table 4. Crystal parameters, data collection information and single-crystal structure refinement
 313 details for correianevesite

314

Formula	$(\text{Fe}^{2+}_{0.72}\text{Mn}^{2+}_{0.20}\text{Fe}^{3+}_{0.08})(\text{Mn}_{1.48}\text{Fe}^{2+}_{0.52})(\text{PO}_4)_2[(\text{H}_2\text{O})_{2.92}(\text{OH})_{0.08}]$
Formula weight	410.01
Crystal system, space group	Orthorhombic, <i>Pbna</i> (no. 60)
<i>Z</i>	4
<i>a</i> , <i>b</i> , <i>c</i> (Å)	9.48871(16), 10.11494(17), 8.70624(16)
<i>V</i> (Å ³)	835.61(3)
<i>F</i> (000)	801
Density ρ_{calc} (g·cm ⁻³)	3.259(8)
Absorption coefficient μ (mm ⁻¹)	5.199
Crystal dimensions (mm)	0.19 × 0.32 × 0.38
Diffractometer	Xcalibur S CCD
λ (Mo- <i>K</i> α) (Å), <i>T</i> (K)	0.71073, 293
Collection mode	(full) sphere
θ range for data collection(°)	3.18 - 34.94
<i>h</i> , <i>k</i> , <i>l</i> ranges	-15 ≤ <i>h</i> ≤ 15, -16 ≤ <i>k</i> ≤ 16, -13 ≤ <i>l</i> ≤ 13
Reflections collected	20430
Unique reflections	1781 ($R_{\text{int}} = 0.0341$)
Reflections with $I > 2\sigma(I)$	1662

Structure solution	direct methods
Refinement method	full-matrix least-squares on F^2
Weighting parameters a, b	0.0174, 0.3503
Extinction coefficient	0.0047(4)
No. of refined parameters	90
Final R indices [$I > 2\sigma(I)$]	$R1 = 0.0176$, $wR2 = 0.0417$
R indices (all data)	$R1 = 0.0204$, $wR2 = 0.0430$
GoF	1.134
$\Delta\rho_{\min}$, $\Delta\rho_{\max}$ ($e/\text{\AA}^3$)	-0.31, 0.42

315
 316
 317
 318

Table 5. Site coordinates and thermal displacement parameters (\AA^2) of atoms for correianevesite.

Atom	x/a	y/b	z/c	U_{eq}
$M(1) = \text{Fe}_{0.80}\text{Mn}_{0.20}$ ^a	0.0	0.0	0.0	0.00978(6)
$M(2) = \text{Mn}_{0.74}\text{Fe}_{0.26}$ ^a	0.065331(19)	0.097199(18)	0.63633(2)	0.01010(5)
P	0.20457(3)	0.10607(3)	0.29198(3)	0.00713(6)
O(1)	0.21646(9)	0.25363(8)	0.33350(11)	0.01207(15)
O(2)	0.10430(9)	0.03779(9)	0.40585(10)	0.01146(15)
O(3)	0.35133(9)	0.04233(9)	0.30005(10)	0.01229(16)
O(4)	0.14828(10)	0.09733(9)	0.12677(10)	0.01383(17)
Ow(1)	-0.09290(17)	0.25	0.5	0.0198(3)
H	-0.139(3)	0.191(3)	0.454(3)	0.055(8) ^b
Ow(2)	-0.02810(10)	0.32654(9)	0.14686(10)	0.01156(15)
H(1)	0.018(3)	0.252(3)	0.134(3)	0.052(8) ^b
H(2)	-0.113(3)	0.287(3)	0.159(3)	0.054(7) ^b

319
 320
 321

^a Fixed during the refinement

^b U_{iso}

322 Table 6. Anisotropic displacement parameters (in Å²) for correianevesite
 323

Atom	U_{11}	U_{22}	U_{33}	U_{23}	U_{13}	U_{12}
M(1)	0.01124(11)	0.00880(11)	0.00930(10)	-0.00005(8)	-0.00259(8)	-0.00117(8)
M(2)	0.01149(9)	0.00988(9)	0.00894(8)	-0.00086(5)	0.00013(6)	-0.00265(6)
P	0.00643(12)	0.00743(12)	0.00752(12)	-0.00028(9)	0.00035(9)	-0.00037(9)
O(1)	0.0116(4)	0.0077(3)	0.0169(4)	-0.0014(3)	0.0000(3)	0.0000(3)
O(2)	0.0109(3)	0.0133(4)	0.0103(3)	0.0003(3)	0.0024(3)	-0.0036(3)
O(3)	0.0088(3)	0.0125(4)	0.0155(4)	-0.0015(3)	0.0004(3)	0.0027(3)
O(4)	0.0150(4)	0.0183(4)	0.0082(3)	-0.0002(3)	-0.0019(3)	-0.0040(3)
Ow(1)	0.0208(7)	0.0171(6)	0.0216(7)	-0.0045(5)	0.000	0.000
Ow(2)	0.0114(4)	0.0093(4)	0.0140(4)	-0.0003(3)	-0.0001(3)	-0.0012(3)

324
 325
 326
 327

Table 7. Selected interatomic distances (Å) in correianevesite.

M(1) – O(4) 2.0413(9) × 2	M(2) – O(1) 2.0981(9)		
– Ow(2) 2.1873(9) × 2	– O(2) 2.1270(9)		
– O(3) 2.2812(9) × 2	– O(2) 2.1424(9)		
<M(1) – O> 2.170	– O(3) 2.1562(9)		
	– Ow(2) 2.2235(9)		
P – O(3) 1.5362(9)	– Ow(1) 2.4600(10)		
– O(4) 1.5369(9)	<M(2) – O> 2.201		
– O(2) 1.5379(9)			
– O(1) 1.5399(9)			
<P – O> 1.5377			
Hydrogen bonds ^a			
Ow(1) – H	0.84(2)	Ow(1) – H···O(4)	3.104(4)
Ow(2) – H(1)	0.88(3)	Ow(2) – H(1)···O(4)	2.865(5)
Ow(2) – H(2) ^b	0.90(3)	Ow(2) – H(2)···O(1)	2.539(5)

328 ^a O-H distances were refined without restraints.

329 ^b Possibly bifurcated H-bond H(2)···O(3) with Ow(2)···O(3) distance of 3.128 Å.

330
 331
 332

Table 8. Dominant components in cationic sites of reddingite-group minerals.

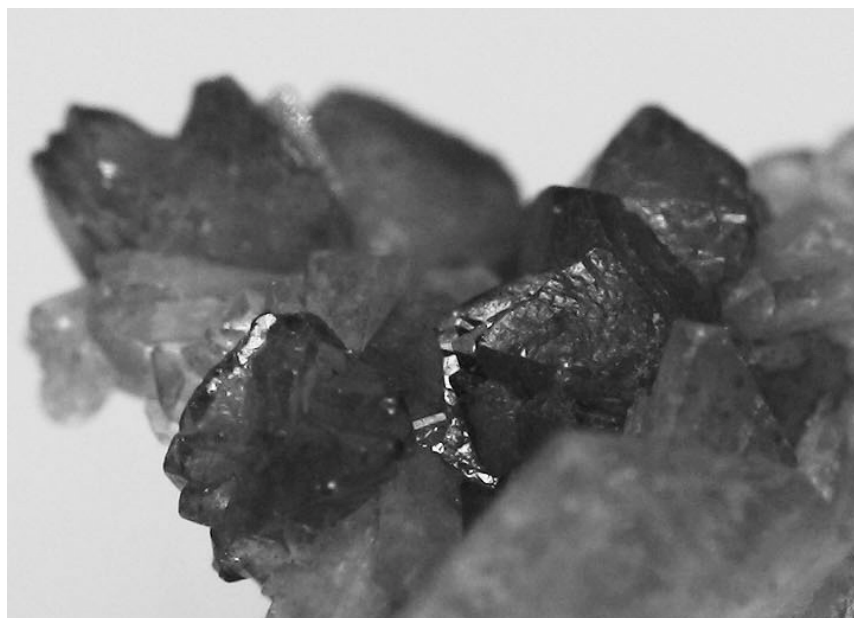
Mineral	M(1)	M(2)
Reddingite	Mn ²⁺	Mn ²⁺
Phosphoferrite	Fe ²⁺	Fe ²⁺
Landesite	Fe ³⁺	Mn ²⁺
Kryzhanovskite	Fe ³⁺	Fe ³⁺
Garyanselite	Mg	Fe ³⁺
Correianevesite	Fe ²⁺	Mn ²⁺

333
 334

335 Table 9. Comparative data for correianevesite and related reddingite-group minerals.
 336

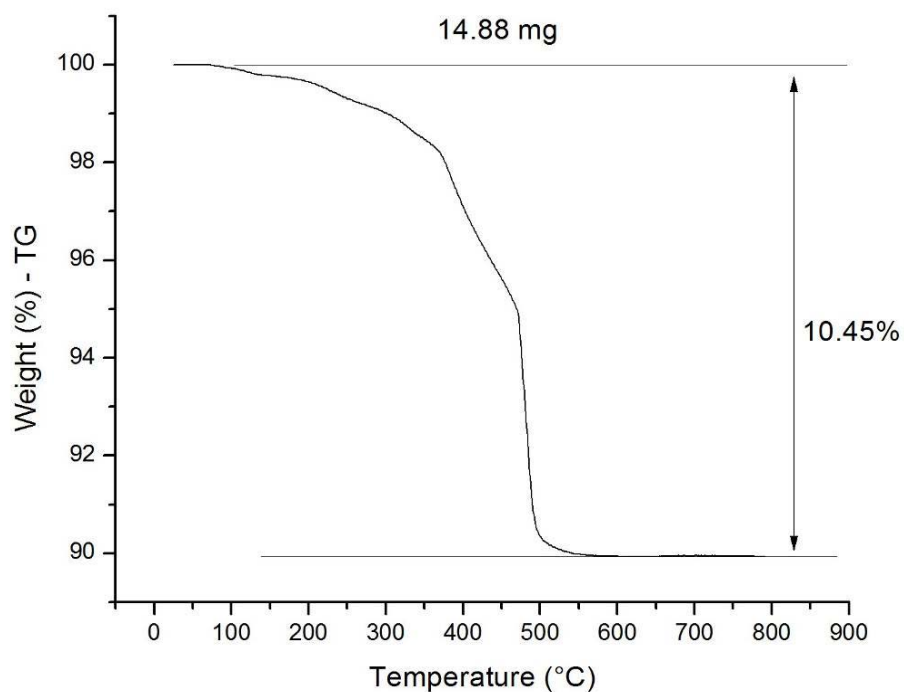
	Correianevesite	Reddingite	Phosphoferrite	Landesite
Formula	$\text{Fe}^{2+}\text{Mn}^{2+}_2(\text{PO}_4)_2 \cdot 3\text{H}_2\text{O}$	$\text{Mn}^{2+}\text{Mn}^{2+}_2(\text{PO}_4)_2 \cdot 3\text{H}_2\text{O}$	$\text{Fe}^{2+}\text{Fe}^{2+}_2(\text{PO}_4)_2 \cdot 3\text{H}_2\text{O}$	$\text{Fe}^{3+}\text{Mn}^{2+}_2(\text{PO}_4)_2 (\text{OH}) \cdot 2\text{H}_2\text{O}$
Space group	<i>Pbna</i>	<i>Pbna</i>	<i>Pbna</i>	<i>Pbna</i>
<i>a</i> , Å	9.4887	9.489-9.49	9.460	9.458
<i>b</i> , Å	10.1149	10.08-10.126	10.024	10.185
<i>c</i> , Å	8.7062	8.70-8.710	8.670	8.543
<i>Z</i>	4	4	4	4
Strong lines of the X-ray powder-diffraction pattern: <i>d</i> , Å (<i>I</i> , %)	5.08 (43) 4.761 (21) 4.314 (28) 3.220 (100) 3.125 (25) 2.756 (35) 2.686 (25) 2.436 (22) 2.233 (23)	4.28 (70) 3.20 (100) 2.737 (80) 2.657 (70) 2.422 (70) 2.234 (70) 1.625 (70)	4.25 (70) 3.18 (100) 2.724 (80) 2.639 (70) 2.408 (70) 2.222 (70) 1.615 (70)	5.096 (54) 4.284 (27) 3.207 (100) 3.163 (35) 3.090 (23) 2.758 (29) 2.630 (24)
Optical data: α β γ Optical sign, $2V$, °	1.661(5) 1.673(5) 1.703(5) (+) 70(10)	1.643 – 1.658 1.648 – 1.664 1.674 – 1.685 (+) 41 – 80	1.663 – 1.672 1.674 – 1.680 1.699 – 1.700 (+) 66 – 70	1.720 1.728 1.735 (-) large
Density, g cm^{-3}	3.25 (meas) 3.275 (calc)	3.10 – 3.24 (meas) 3.26 (calc)	3.10 – 3.29 (meas) 3.32 (calc)	3.026 – 3.03 (meas) 3.210 (calc)
Mohs hardness	3½	3-3½	3-4½	3-3½
References	This work	Tennyson (1954); Kleber and Donnay (1961); Feklichev (1989); Frost et al. (2012)	Tennyson (1954); Kleber and Donnay (1961); Moore and Araki (1976); Moore (1971); Moore et al. (1980); Feklichev (1989)	Moore (1964); Moore et al. (1980); Feklichev (1989)

337
 338



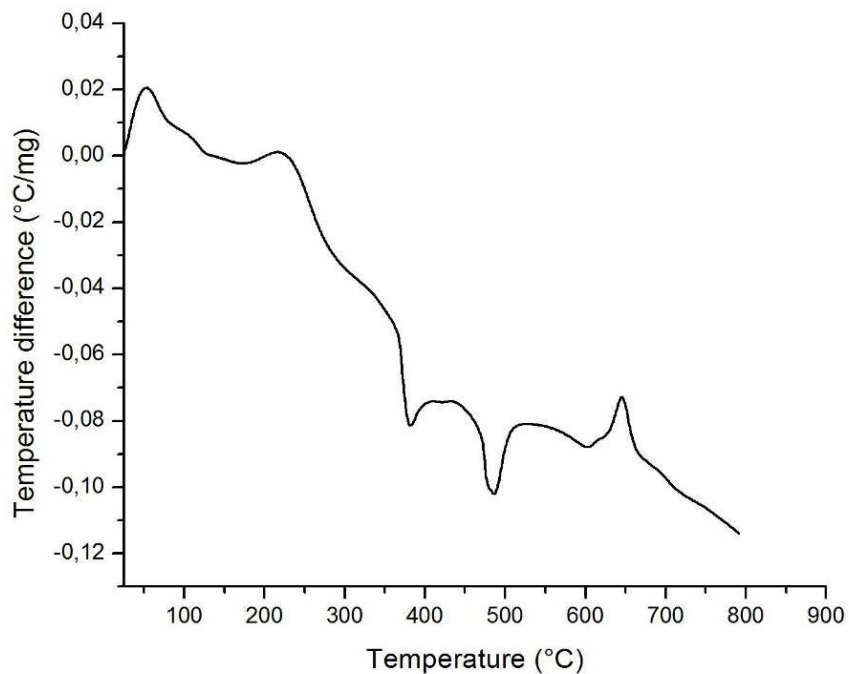
339
340
341
342

Figure 1. Bipyramidal crystals of correianevesite on hureaulite. Field of view: 6 mm. Photo: Carlos Menezes.



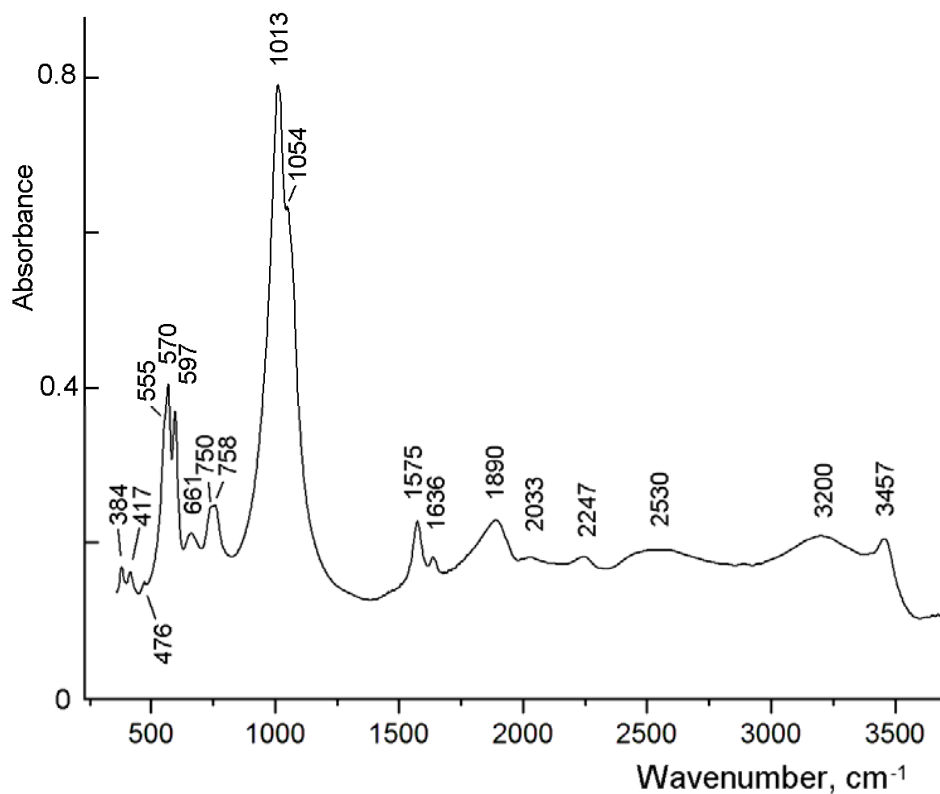
343
344
345
346
347

Figure 2. TG curve of correianevesite obtained in nitrogen atmosphere at a heating rate of $10^{\circ}\text{C min}^{-1}$.



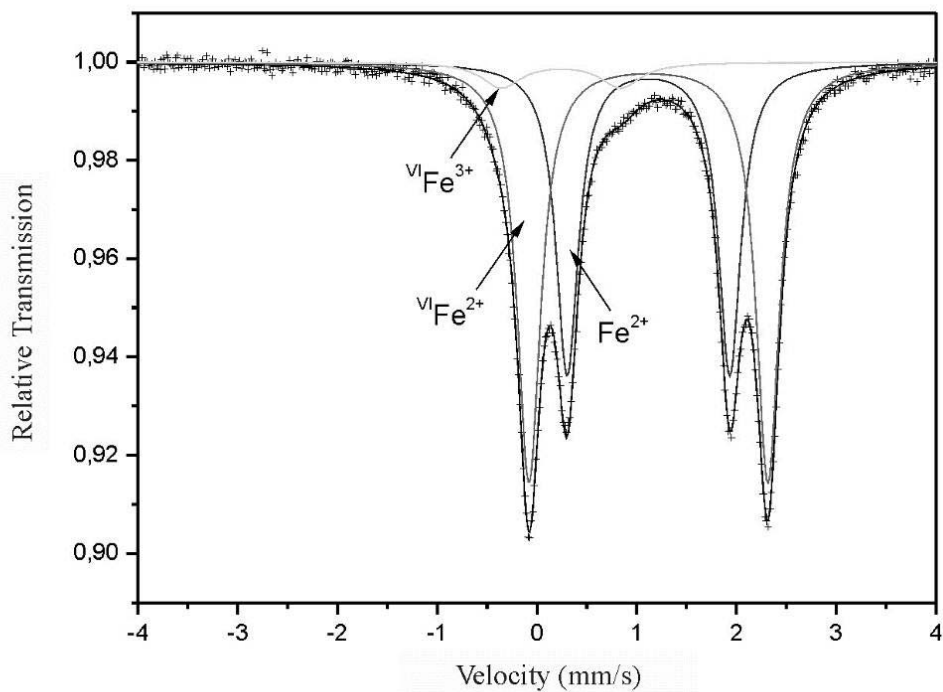
348
349
350
351

Figure 3. DTA curve of correianevesite obtained in nitrogen atmosphere at a heating rate of $10^{\circ}\text{C min}^{-1}$.



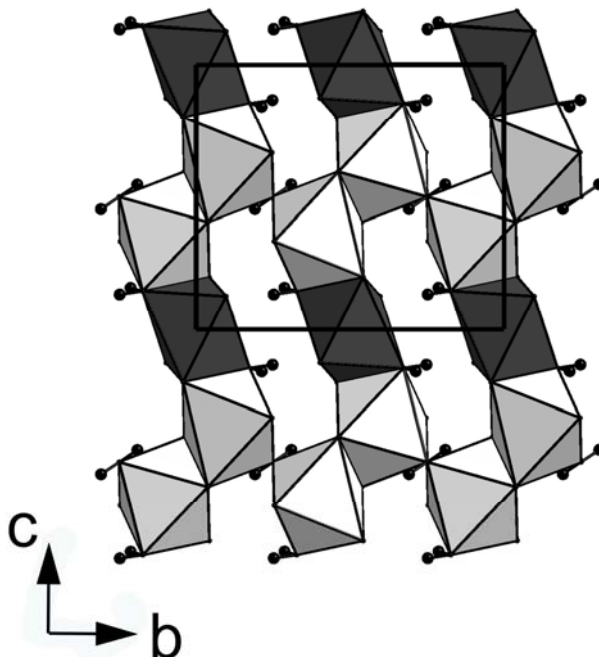
352
353
354

Figure 4. IR spectrum of powdered correianevesite in KBr pellet.



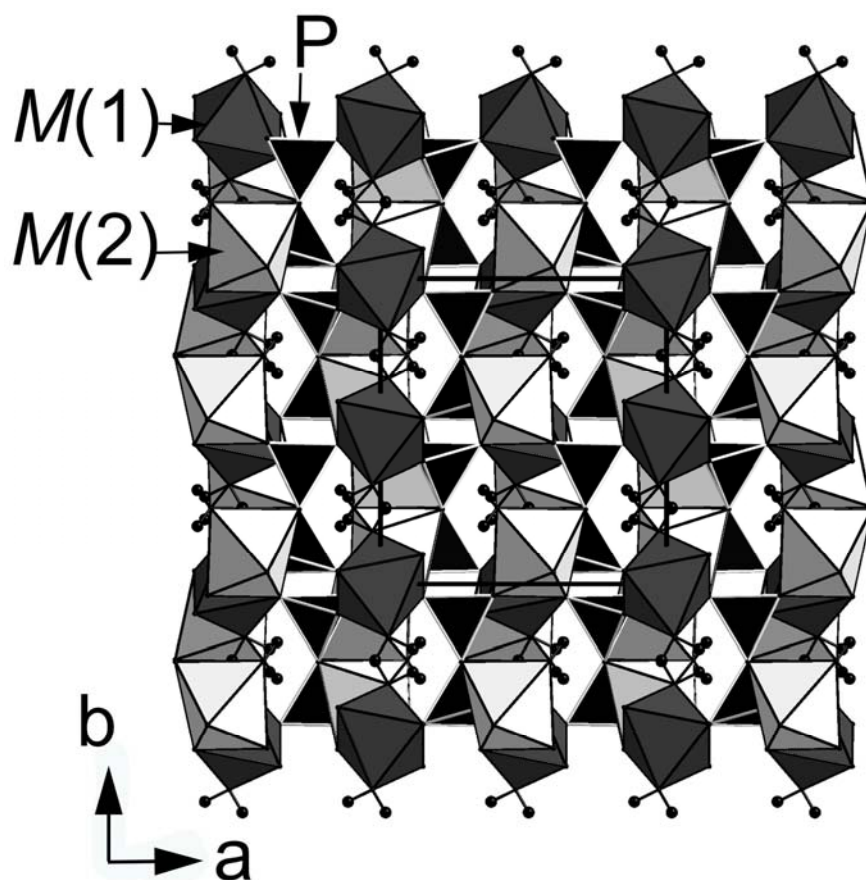
355
356

Figure 5. Mössbauer spectrum of correianevesite.



357
358
359
360

Figure 6. Octahedral layer in the structure of correianevesite. $M1O_6$ octahedra are dark, $M2O_6$ octahedra are light, H atoms are shown with small circles. Unit cell is outlined.



361
362

Figure 7. The crystal structure of correianevesite: ab projection. Unit cell is outlined.